University of Pisa
Clinical Pathology Specialization School

EFFECTS OF IN VIVO 3-IODOTHYRONAMINE ADMINISTRATION ON GENE EXPRESSION IN ADIPOSE TISSUE.

Candidate
Dr.Veronica Mariotti

Supervisor
Prof. Riccardo Zucchi

INDEX

ABSTRACT

Thyroid hormones (THs) control the adipose tissue development and metabolism. They regulate both adipocyte proliferation and differentiation and, as they cause weight loss by increasing the metabolic rate, may be useful for obesity treatment. However, due to their cardiotoxic effects, like tachycardia and arrhythmia, their use is limited to hypothyroid obese patients. Some TH metabolites have been recently shown to possess the same beneficial metabolic effects as THs without the same negative effects. A biogenic amine named 3-Iodothyronamine (T_1AM), i.e., is an endogenous compound derived by thyroxine (T_4) deiodination and decarboxylation that affects carbohydrate and lipid metabolism without undesirable side effects. T_1AM exhibits cardiac effects opposite to those associated with thyroid hormones, like bradycardia in mice, and in isolated working rat heart, it produces a rapid, reversible, dose-dependent decrease in cardiac output, aortic pressure and coronary flow. These findings suggest that T_1AM produces a negative inotropic and chronotropic effect.

Intraperitoneal injections of T_1AM also induce reduction of RQ from 0.9 to 0.7, both in mice and Djungarian hamsters. This indicates that carbohydrate utilisation is reduced in response to T_1AM and energy requirements are covered by lipid utilisation. Interestingly, the complete RQ shift is reached 4.5 h after the T1AM injection and persists at least for 24 hours. Ketone bodies in the urine and the significant loss of body fat mass confirm that lipids are predominantly used to cover the energy requirements in response to T_1AM administration.

The molecular mechanisms by which T_1AM favours lipid than glucose catabolism are not known, but changes in gene expression can be hypothesized, given the delayed and long lasting phenotypical effects of T1AM.

To verify this hypothesis we analyzed by microarrays the gene expression profiles in subcutaneous adipose tissues of eight rats chronically treated with T_1AM as compared with eight untreated rats.

Many genes linked to lipid metabolism, adipogenesis and angiogenesis appeared affected by chronic administration of T_1AM, thus explaining, at least in part, the T_1AM phenotypic effects observed in rodents. Furthermore, T_1AM influenced the expression of several genes relating to lipoprotein metabolism that provide new insights on T_1AM mechanism of action, like, i.e., the regulation of cholesterol homeostasis.

INTRODUCTION

Thyroid hormones (THs) control the adipose tissue development and metabolism (Viguerie et al. 2002). They regulate adipocyte proliferation and differentiation (Hauner et al. 1989, Darimont et al. 1993) and, as they cause weight reduction loss by increasing the metabolic rate, may be indicated for obesity treatment (Krotkiewski 2002). Their use, however, is limited because they produce thyrotoxic effects including cardiotoxic effects like tachycardia and arrhythmia (Krotkiewski 2002). The identification of TH analogs that retain anti-obesity efficacy with a few undesirable side effects is therefore an important research goal. Some TH metabolites have been recently shown to possess the same beneficial metabolic effects as THs without the same negative effects. The biogenic amine 3-Iodothyronamine (T_1AM) for example, affects carbohydrate and lipid metabolism without undesirable side effects (Chiellini et al. 2007, Braulke et al. 2008). Scanlan and collaborators by using synthetic T_1AM as a standard in liquid chromatography/tandem mass spectrometry (LC-MS/MS) assay, demonstrated that T_1AM is an endogenous component of biogenic amine (Scanlan et al. 2004). It has been detected in rat serum and tissues as well in human and Djungarian hamster blood (Braulke et al. 2008, Saba et al. 2010). The quantitative analysis of its physiological concentration has indicated that T_1AM content is higher in organs than in blood suggesting that some tissues are able to accumulate it (Saba et al. 2010).

1. T1AM

1.1. T_1AM BIOSYNTHESIS

The pathway of endogenous T_1AM biosynthesis is still unknown. It has been suggested that T_1AM derives from THs through decarboxylation and deiodination (Scanlan et al. 2004). Although the iodothyronine-decarboxylating enzyme has not been still identified (Wu et al. 2005). T_1AM might be formed by decarboxylation of T_4 and rT_3, to T_4AM and rT_3AM respectively. T_4AM is a good substrate for Dio_3 and is deiodinated to rT_3AM. The sequential deiodination of rT_3AM by Dio_1 and Dio_2 produces T_1AM (Piehl et al. 2008) (figure 1). However, no direct evidence of T_4 or T_3 conversion to T_1AM is known at present.

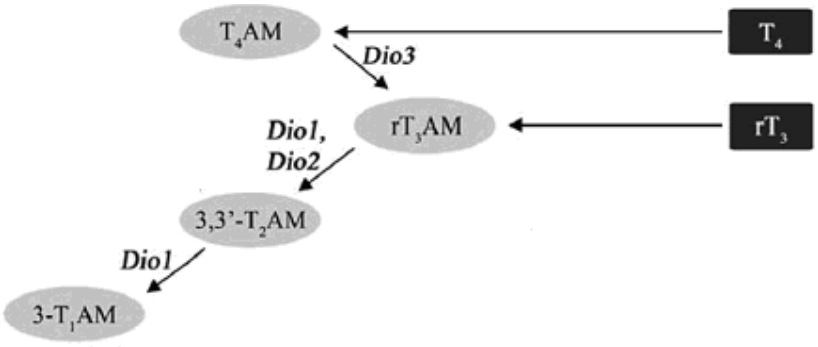

Figure 1. Pathways suggested for T_1AM biosynthesis. *Diagonal arrows*, deiodination reactions catalyzed by deiodinases . *Horizontal arrows*, putative decarboxylation reactions that might represent the first step of T_1AM biosynthesis.

1.2. T_1AM METABOLISM

T_1AM is substrate for sulfotransferases (SULTs) and $SULT_{1A2}$, $SULT_{1A3}$ and $SULT_{1E1}$ show the highest activity toward T_1AM. It has been hypothesized that SULT action reduces and regulates the T_1AM effects (Pietsch, Scanlan and Anderson 2007). In 2009, Wood and colleagues demonstrated that T_1AM is susceptible to oxidative deamination of the ethylamine side chain by an amine oxidase that converts it in thyroacetic acid (TA_1) whose biological activity is unknown (Wood et al. 2009).

1.3. T_1AM RECEPTORS

The G protein-coupled trace amine-associated receptor 1 (TAAR1) is the first molecular target suggested to mediate the T_1AM effects. T_1AM induces the synthesis of cAMP in HEK-293 cells stably transfected with rat TAAR1 (Scanlan TS et al., 2004). However, T_1AM also inhibits the cAMP synthesis through the interaction with the α_{2A} adrenergic receptor ($Adra_{2A}$), a $G_{\alpha i}$ coupled receptor expressed in many cell types (Regard et al. 2007). Both these receptors interact with T_1AM and the final effect depends on TAAR1/ $Adra_{2A}$ ratio.

T_1AM, moreover, inhibits vesicular monoamine transporter (VMAT2), an intracellular transporter that packages monoamine into synaptic vesicles. This observation is suggestive of a neuromodulatory role for T_1AM (Snead et al. 2007).

1.4. T_1AM INTRACELLULAR TRANSPORT

T_1AM has been recently found to be largely bound to the apoB-100-containing lipoproteins in human serum. It reversibly binds the apoB-100-containing lipoprotein with an equilibrium dissociation constant of 17 nM and T_1AM /apoB-100 stoichiometry of 1:1. This binding is highly selective for T_1AM and increases its intracellular uptake significantly (Roy, Placzek and Scanlan 2012).

A 2009 study demonstrated that the intracellular transfer of T_1AM occurs in multiple cell lines and involves a specific mechanism of transport that can be saturated and inhibited. T_1AM transport is independent from sodium and chloride and is driven by an outwardly directed proton gradient. By using a library of siRNA against the entire solute carrier (SLC) superfamily of 403 transporter genes, eight putative T_1AM transporters were identified. These transporters collectively participate in the regulation of T_1AM intracellular levels (Ianculescu, Giacomini and Scanlan 2009).

T_1AM uptake is also mediated by non-SLC transporters or by receptor-mediated endocytosis (Lin and Scanlan 2005).

1.5. T_1AM EFFECTS

Intraperitoneal (ip) injections of T_1AM in C57BL/6 wild-type mice or Djungarian hamsters induce numerous effects like bradycardia, hypothermia, hyperglycemia, decrease of metabolic rate ($\dot{V}O_2$), reduction of respiratory quotient (RQ), ketonuria and loss of fat mass (Scanlan et al. 2004, Braulke et al. 2008, Regard et al. 2007) (table 1). In Djungarian hamsters, the injection of 50mg T_1AM/kg leads to a 10-fold increase of T_1AM blood concentration, from 6 nM to 56 nM, (Braulke et al. 2008) whose origin is unclear whether is pharmacological or physiological.

Most of T_1AM effects are detected within minutes after the injection. The bradycardia, hyperglycemia, hypothermic and hypometabolic state reach a maximum in 1-2 h, while the complete RQ shift is reached 4.5 h after the T_1AM injection. Afterwards, heart activity, metabolic rate, body temperature and blood glucose levels return to baseline values within 6-8 h, while the reduced RQ persists for at least 24 h. Ketonuria and the loss of fat mass appear and revert much later (Scanlan et al. 2004, Braulke et al. 2008, Regard et al. 2007).

	Experimental model	Mechanism and/or interpretation
Central nervous effects		
Hypothermia	C57BL/6 mice, Djungarian hamsters	Due to a decrease in metabolic rate
Inhibition of monoamine transporters	Transfected cell lines	Hypothesized action as a physiologically relevant neuromodulator
Cardiac effects		
Negative chronotropy,[a] negative inotropy	C57BL/6 mice, isolated rat hearts	Due to effects on intracellular calcium homeostasis
Effects on plasma hormone concentrations		
Hyperglycemia, hypoinsulinemia, hyperglucagonemia	Primary human and murine pancreatic β-cells, male Wistar rats, ROSA26PTX mice	Hypothesized central action increasing the sympathetic tone on pancreatic islets
Hypothalamic-pituitary-thyroid-axis: TSH ↓, T_4 ↓, T_3 ↓	Male Wistar rats	Causing a state reminiscent of the nonthyroidal illness
Metabolic effects		
Metabolic rate ↓, RQ ↓, lipid utilization ↑, fat mass ↓, ketonuria	C57BL/6 mice, Djungarian hamsters	Hypothesized action as a physiologically relevant modulator of metabolism: change in metabolic fuel utilization from carbohydrates to mainly lipids

Table 1. Summary of the T_1AM effects. ↑, Increase; ↓, Reduction.

1.5.1 Hypothermic and hypometabolic state

After T_1AM injection into C57BL/6 wild-type mice and Djungarian hamsters body temperature and metabolic rate decrease within minutes. The body temperature falls from 37 to 31°C within 30 min and 90 min later it drops to 29.5°C. The metabolic rate, measured as decrease in VO_2, declines from 2.5 to 1.8 ml/gh within 5 min. Both these effects are reversible: the animals recover from hypothermia and hypometabolism 6-8 h after the T1AM administration (Braulke et al. 2008, Scanlan et al. 2004). Noteworthy, the hypothermia is preceded by the decrease in metabolic rate and the hypothermic effect is interpreted as a result of the reduced metabolic rate (Braulke et al. 2008).

1.5.2 Negative chronotropy and inotropy

The administration of T_1AM to C57BL/6 wild-type mice induces reversible bradycardia: the heart rate drops from 600 to 350 beats per minute and reverts to normal 6-8 h after the injection (Scanlan et al. 2004). In isolated working rat hearts perfused with increasing T_1AM concentrations, the heart rate decreases within minutes to an IC_{50} of 37 µM. It also causes the fall of cardiac output to an IC_{50} of 29 µM. Both these effects persist for the whole duration of the perfusion and revert to normal by removing T_1AM (Chiellini et al. 2007).

These findings suggest that T_1AM produces a negative inotropic and chronotropic effect.

T_1AM also inhibits other cardiac parameters including the aortic pressure and the coronary flow (Chiellini et al. 2007).

1.5.3 Hyperglycemia

In 2007 Regard and colleagues observed that T_1AM acts as a regulator of insulin secretion (Regard et al. 2007). The ip administration of 50mg/kg of T_1AM, in fact, increases blood glucose levels in C57BL/6 wild-type mice. This effect is detectable within minutes after the injection, reaches a maximum of 250% of the basal value 2h after the treatment and reverts 8 h later. It is accompanied by a decrease in blood insulin levels and an increase in blood glucagon levels. The administration of insulin normalizes the blood glucose levels, indicating that peripheral tissues remain sensitive to insulin during the T_1AM treatment (Regard et al. 2007). According to these findings T_1AM has been observed to inhibit the release of insulin from primary murine and human pancreatic ß-cells in vitro (Regard et al. 2007).

More recently it has been reported that intracerebroventricular (icv) infusion of a 100-fold lower dose of T_1AM (0.5mg/kg) produces even more pronounced effects on peripheral glucose metabolism in male Wistar rats (Klieverik et al. 2009).

1.5.4 Reduction of the respiratory quotient, ketonuria and loss of fat mass

In both C57BL/6 wild-type mice and Djungarian hamsters, an ip injection of T_1AM induces a reduction of RQ from 0.9 to 0.7 (Braulke et al. 2008). This indicates that the utilisation of carbohydrates is suppressed in response to T_1AM and that the energy requirements are covered by lipid consumption (Braulke et al. 2008). Interestingly, the complete RQ shift is reached 4.5 h after the injection and persists for at least 24 h (Braulke et al. 2008). The presence of ketone bodies in the urine and the significant loss of body fat mass confirm the assumption that lipids are predominantly used to cover the energy requirements in response to T_1AM treatment (Braulke et al. 2008).

1.5.5 Other effects

Dhillo and colleagues demonstrated that T_1AM affects the food intake (Dhillo et al. 2009). Several hypothalamic nuclei like the paraventricular nucleus and arcuate nucleus are important regulators of food intake and energy balance. Given that T_1AM is present in the brain and TAAR1 is expressed in the hypothalamic nuclei these authors hypothesized that T_1AM plays a role in regulating the energy homeostasis. They observed that ip or iv injections of low doses of T_1AM (4 and 1.2 µmol/kg, respectively) induced food intake without affecting the metabolic rate and the locomotor activity in rats and mice (Dhillo et al. 2009). However, at higher doses of T_1AM (50mg/kg) the authors confirmed the previously reported reduction of oxygen

consumption and locomotor activity (Braulke et al. 2008). In addition, T_1AM injected directly into the arcuate nucleus of rodents caused a 3-fold increase in food intake, suggesting that T_1AM is an orexigenic compound that acts through the arcuate nucleus to increase the food intake (Dhillo et al. 2009).

In hypothyroid rats T_1AM produces relevant effects on O_2 consumption and ROS production by liver mitochondria. In particular, T_1AM reduces oxygen consumption in mitochondria and increases H_2O_2 release. This suggests that the electron flow rate along the respiratory chain decreases in presence of T_1AM (Venditti et al. 2011).

2. GENE EXPRESSION MICROARRAY

The microarray technology, introduced in 1995 by a research group of Standford University (Schena et al. 1995), is a highthroughput technology which provides a global view of gene expression patterns in biological samples. By the simultaneous evaluation of the expression levels of thousands of genes, the microarrays allow users to compare two biological samples (normal VS pathological or treated VS control sample) in order to obtain information on the molecular mechanisms responsible for their phenotype.

On a solid surface thousands of single strand oligonucleotide sequences (probes) are immobilized, ready to hybridize to complementary sequences (targets) extracted from the biological samples of interest. Each gene is represented by thousands of identical probes within a feature (spot) and a single microarray contains up to tens of thousands of spots (Figure 2).

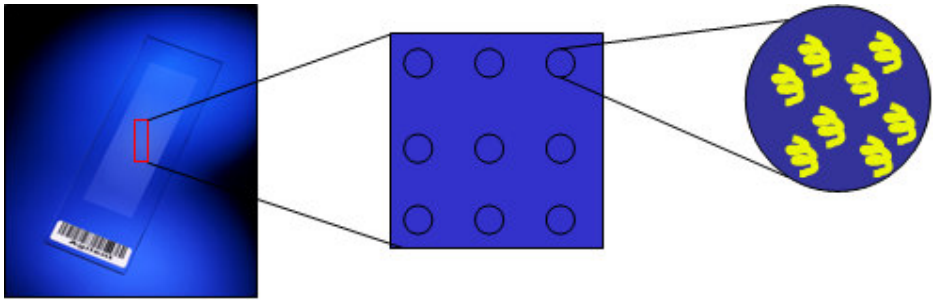

Figure 2. Schematic representation of a microarray slide. A microarray consists of multiple features (spots). Each spot is representative of a gene and contains thousand of identical probes (yellow helices).

In a typical dual-color microarray experiment total RNA is extracted from the two samples to be compared. The RNA is converted in cDNA by reverse transcription polymerase chain reaction. The cDNA of each sample is then labelled with a different fluorescent dye, for example one with Cy_3 (green) and the other with Cy_5 (red). The two labelled cDNAs are mixed in the same quantity and deposited on the microarray slide. After an overnight incubation the sequences of labelled cDNAs (targets) hybridize to complementary sequences attached on the array (figure 3).

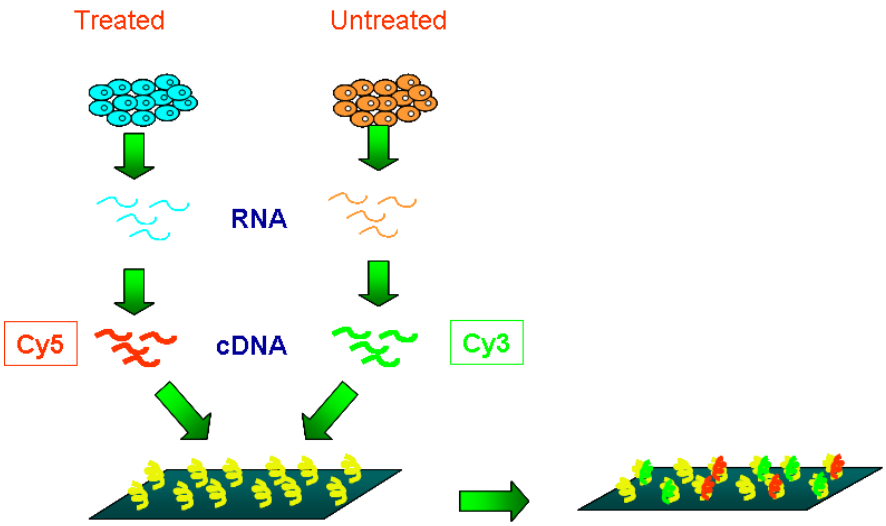

Figure 3. Schematic representation of a dual-color microarray experiment.

The scanning of the microarray surface with a double laser scanner enables to highlight the fluorescent spots and produces two images. In the first image the Cy_3 fluorescence is displayed as green and in the second the Cy_5 fluorescence is displayed as red (figure 4). The overlapping of the two images produces a single image that is processed to subtract the background fluorescence and to normalize the obtained data.

The measured red and green fluorescence intensities for each spot are proportional to the amount of mRNA, corresponding to a specific transcript, expressed by the two compared samples.

For each spot the two fluorescence intensities are translated into numerical values whose ratio indicates the difference in the expression of each gene between the two samples. A statistical analysis is then performed to identify those genes whose differential expression is statistically significant between the two samples of interest.

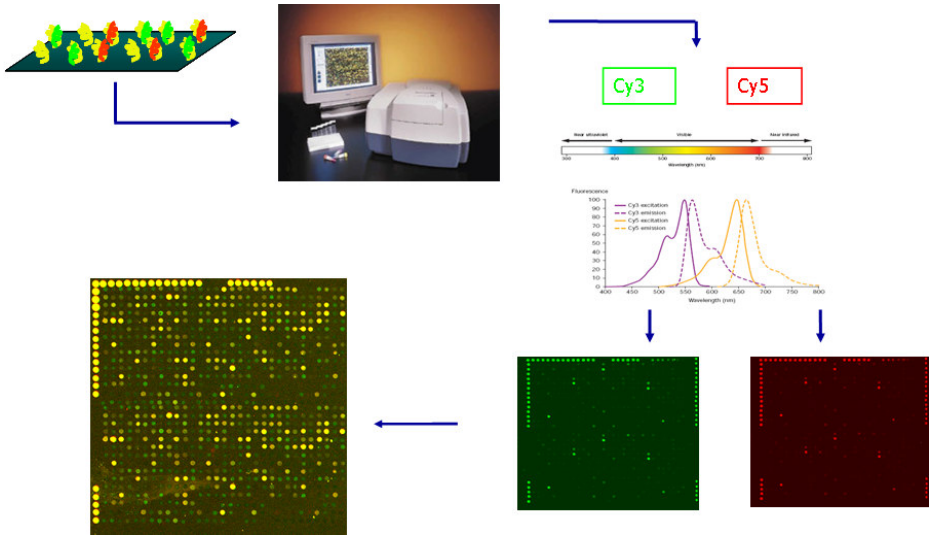

Figure 4. Image acquisition of dual-color microarray. The double laser scanner performs a double scanning and produces two distinct images for each fluorescent dye. The two images are overlapped to obtain a single image.

3. AIM OF THE STUDY

T_1AM slows down the metabolism by blocking carbohydrates utilisation and promoting lipid consumption. The molecular mechanisms by which T_1AM favours the lipid catabolism over glucose catabolism is not known. As the T_1AM effects on fatty acid metabolism outlast all the other effects (bradycardia, hyperglycemia, hypothermia and hypometbolism) it is reasonable to expect that the regulation of energy utilization by T_1AM derives from changes in gene expression. To verify this hypothesis we used the microarray technology and analyzed gene expression profiles in the adipose tissue of rats chronically treated with T_1AM as compared to untreated rats.

MATERIALS AND METHODS

ANIMALS AND T_1AM TREATMENT

The animals used in this study were male Wistar rats. Prior to any experimental manipulation the rats were acclimatized for one week in the animal house facility at the Human and Environmental Science Departement of Pisa University.

The project was approved by the Animal Care and Use committee of the University of Pisa.

Eight rats of about 100–125 g body weight were treated with T_1AM by intraperitoneal injection of 10 mg /Kg twice a day for five days. Eight control rats were treated with T_1AM free-intraperitoneal injection under parallel housing conditions. The rats were sacrificed by guillotine and the subcutaneous adipose tissue was immediately removed. The tissue samples were flash-frozen and stored at -80°C until their use.

ISOLATION, AMPLIFICATION AND LABELLING OF RNA

Total RNA was isolated from adipose tissues by the RNeasy Lipid Tissue Mini kit (Qiagen, Valencia, CA, USA).

Residual DNA was eliminated by on-column DNase digestion using the RNase-Free DNAase Set (Qiagen, Valencia, CA, USA).

The quantity and purity of total RNA were measured by 260 nm UV absorption and by 260/280 ratio, respectively, using a NanoDrop ND-1000 Spectrophotometer (NanoDrop Technologies, Wilmington, DE, USA). All RNAs displayed a 260/280 optical density ratio $\geq$1.9.

The RNA integrity was checked with the Agilent 2100 Bioanalyzer (Agilent Technologies, Palo Alto, CA, USA) using the Agilent RNA 6000 Nano kit (Agilent Technologies, Palo Alto, CA, USA). All RNAs displayed a RNA Integrity Number (RIN) $\geq$8.

One microgram of total RNA from treated and control animals was amplified and labelled with Cyanine 5 (Cy5) and Cyanine 3 (Cy3) dyes (Agilent Technologies, PaloAlto, CA, USA), respectively, by the Quick-Amp Labeling kit (Agilent Technologies, Palo Alto, CA, USA). In order to monitor the experiment, from sample amplification and labelling to microarray hybridization, a RNA Spike-In (Agilent Technologies, PaloAlto, CA, USA) was added to each RNA sample.

The Cy3 and Cy5 dye incorporation rates were measured by UV absorption at 555 nm and 647 nm, respectively.

Both fluorophores showed a comparable incorporation efficiency ranging between 11 and 15 pmol of dye per µg of amplified RNA.

MICROARRAY HYBRIDIZATION

The hybridization mixture containing 825 ng of Cy3-labelled amplified RNA (corresponding to 9-10 pmol of Cy3 dye), 825 ng of Cy5-labelled amplified RNA (corresponding to 11-12 pmol of Cy5 dye), 11µl of 10X Blocking Agent, 2.2 µl of 25X fragmentation buffer and 55 µl of 2X GE hybridization buffer (the last three from the Gene Expression hybridisation kit plus, Agilent Technologies, Palo Alto, CA, USA) was hybridized to Whole Rat Genome Oligo Microarrays 4x44K (Agilent Technologies, Palo Alto, CA, USA). Each slide contains 4 arrays with 44,000 60-mer oligonucleotide probes representing 41,012 unique probes.

The array hybridisation was performed at 65°C in the Agilent oven (Agilent Technologies, Palo Alto, CA, USA) for 17 h under constant rotation. After hybridisation, the arrays were washed following the Quick Amp Labeling protocol (Agilent Technologies, Palo Alto, CA, USA). To prevent the ozone-mediated fluorescent signal degradation, the arrays were immersed in Acetonitrile solution (Sigma-Aldrich, St.Louis, MO, USA) for 10 sec and successively in Stabilization and Drying solution (Agilent Technologies, Palo Alto, CA, USA) for 30 sec. These last two washes were performed at room temperature.

MICROARRAY EXPERIMENTAL DESIGN

A balanced block design was applied: on each array, two differently labelled samples from the treated and the control groups were hybridized, for a total of eight arrays (figure 5).

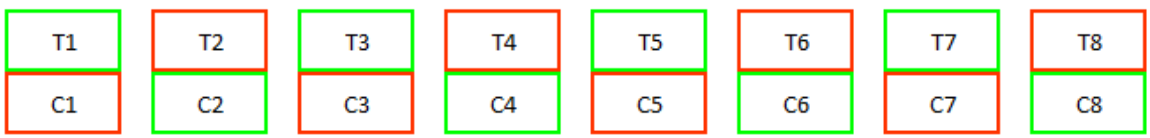

Figure 5. Balanced Block experimental design.

MICROARRAY DATA ACQUISITION AND ANALYSIS

Microarray images were acquired by the Agilent scanner G2565BA (Agilent Technologies, Palo Alto, CA, USA) at 5µm resolution and intensity raw data were extracted by the software Feature Extraction V10.5 (Agilent Technologies, Palo Alto, CA, USA).

Data preprocessing and statistical analysis were performed by LIMMA (LInear Model of Microarray Analysis) package (Smyth 2005). The intensity raw data were background subtracted by the *normexp* method and normalized within-arrays with the *LOESS* and between-arrays with the *scale* methods, respectively.

For the statistical analysis, the bayesian moderated t-statistic (Smyth 2004) was used and only genes with Benjamini and Hochberg (Benjamini and Hochberg 1995) adjusted-p-value < 0.01 were considered as differentially expressed.

Pathway-Express was used to map the differentially expressed genes in KEGG pathways (http://vortex.cs.wayne.edu/projects.htm#Pathway-Express) (Draghici et al. 2007). *GeneCards*® (http://www.genecards.org) (Safran et al. 2003), *Onto-Express* (http://vortex.cs.wayne.edu/ontoexpress/) (Draghici et al. 2003, Khatri et al. 2002), *PubGene* (http://www.pubgene.org/) (Jenssen et al. 2001) and *Coremine* (http://www.coremine.com/medical/) were used to perform an accurate screening of the scientific literature concerning the differentially expressed genes.

MICROARRAY DATA VALIDATION BY RT-QPCR

The same RNA samples used in the microarray experiment were used to perform the RT-qPCR experiments. Total RNAs were reverse transcribed with random and oligo-dT primers by the QuantiTect Reverse Transcription kit (Qiagen, Valencia, CA, USA). PCR primers were designed by the Beacon Designer 4.0 software (Premier Biosoft International, Palo Alto, CA, USA) and synthesized by Sigma-Aldrich (Sigma-Aldrich, St.Louis, MO, USA). The primer sequences are listed in table 2.

RT-qPCR was performed by the iCycler iQ instrument (Biorad, Hercules, CA, USA) using the iQ SYBR Green Supermix (Biorad, Hercules, CA, USA). The amplification protocol was: 3 min at 95°C (DNA polymerase activation), then 40 cycles at 95°C per 30s (denaturation step), 58–62°C (depending on primer Tm) per 60s (annealing step) and 72°C per 30s (extension step). Afterwards, a gradual increase in temperature from 55°C to 95°C at 0.5°C/10s was utilized to

build a melting curve. For each primer pair, the amplification efficiency was tested using five serial dilutions of cDNA carried out in duplicate. To reduce the effects of the biological variation on the amplification efficiency, a cDNA sample obtained by pooling the RNAs from all the eight control samples was used. For all the primer pairs the amplification efficiency was between 90 and 110% and the square regression coefficient (r^2) was >0.99. The stability of six housekeeping genes (Mapk6, Kdm2b, Psmd4, Cypa, B2mg, Bact) was evaluated by using geNorm software (Vandesompele et al. 2002). geNorm identified three housekeeping genes (Psmd4, Cypa and B2mg) as stable (M<1.5 and $V_{3/4}$<0.114), which were used to normalize the expression values of the target genes.

Each sample was run in triplicate to calculate the standard deviation (SD) for the three experimental replicates. Only the experiments with SD < 0.4 for each group of replicates were considered The relative expression levels for the target genes in T_1AM treated respect to T_1AM untreated tissues were calculated by geNorm method and reported as fold increase or decrease.

One- and two-tailed Wilcoxon signed rank tests were applied to evaluate the statistical significance of RT-qPCR results by using a threshold p-value ≤ 0.05.

Housekeeping genes				
Gene Symbol	RefSeq mRNA	Forward Primer	Reverse Primer	Ta
Mapk6	**NM_031622.2**	5'- GCCACACAAACCGCTGAC -3'	5'- CCGTTGGGAAAGAGTAGATGC -3'	58°C
Kdm2b	**NM_001100679**	5'- GCAAGCAAGTCACCAAGG -3'	5'- TCGTTTCAGATTCCAAAGGG -3'	58°C
Psmd4	**NM_031331**	5'- AGATGATGCCCTACTGAAGATGAC -3'	5'- GACGCTCTGAAGGAACTCTGG -3'	58°C
Cypa	**NM_017101**	5'- CAAGACTGAGTGGCTGGATGG -3'	5'- GCTACAGAAGGAATGGTTTGATGG -3'	58°C
B2mg	**NM_012512**	5'- TCAAGTGTACTCTCGCCATCC -3'	5'- GCAAGCATATACATCGGTCTCG-3'	58°C
Bact	**NM_31144**	5'- CCACACCCGCCACCAGTTC-3'	5'- GACCCATACCCACCATCACACC -3'	60°C
Target genes				
Gene Symbol	RefSeq mRNA	Forward Primer	Reverse Primer	Ta
Scarb1	**NM_031541**	5'- GCAGTGATGATGGAGGACAAGCC -3'	5'- GAAGACGGTGAAGACGCCAGAAC -3'	62°C
Hdlpb	**NM_172039.2**	5'- CCATTGCGGTAGAGGTGAAG -3'	5'- ACGGTGAAGCCAGGAAGG -3'	58°C
Igfbp2	**NM_013122**	5'- CCTCTGGAACATCTCTACTC -3'	5'- ACTGGCTGTGGTTTACTG -3'	58°C
Ascl5	**NM_053607**	5'- TGGGATGCTGGGTGTTTG -3'	5'- TACTTCCTGTGTCTTCTCTGG -3'	58°C
Apod	**NM_012777**	5'- AGTTGAGGGTGAAGCCAAACAGAG -3'	5'- GCAGGAATACACGAGGGCATAGC -3'	62°C
Cebpb	**NM_024125**	5'-ATCGACTTCAGCCCCTACCT-3'	5'-GGCTCACGTAACCGTAGTCG-3'	60°C

Table 2. Housekeeping genes, target genes and RT-qPCR primers.

RESULTS

MICROARRAY RESULTS

T_1AM chronic administration altered the gene expression in rat subcutaneous adipose tissue. Specifically, 378 genes were differentially expressed, 268 up-regulated and 110 down-regulated. Due to the limited information on pathways and gene functional annotations currently retrievable from databases, only a small group of genes was mapped by Pathway Express. Specifically, Pathway Express placed 60 differentially expressed genes in 70 pathways (table 3).

To identify other genes that might have an important role in T_1AM molecular mechanism of action, the list of differentially expressed genes was further investigated by an accurate screening of the scientific literature. By using the information included in OntoExpress, GeneCards, PubGene and Coremine bioinformatics tools other 20 genes implicated in relevant mechanisms were identified (table 4).

ENVIRONMENTAL INFORMATION PROCESSING	CELLULAR PROCESSES	ORGANISMAL SYSTEMS	HUMAN DISEASES
Calcium signaling pathway	Adherens junction	Adipocytokine signaling pathway	Acute myeloid leukemia
ECM-receptor interaction	Apoptosis	Antigen processing and presentation	Alzheimer's disease
ErbB signaling pathway	Endocytosis	Axon guidance	Amyotrophic lateral sclerosis (ALS)
Hedgehog signaling pathway	Focal adhesion	B cell receptor signaling pathway	Basal cell carcinoma
MAPK signaling pathway	Gap junction	Chemokine signaling pathway	Bladder cancer
Phosphatidylinositol signaling system	Regulation of actin cytoskeleton	Circadian rhythm	Chronic myeloid leukemia
VEGF signaling pathway	Regulation of autophagy	Complement and coagulation cascades	Colorectal cancer
Wnt signaling pathway	Tight junction	Fc epsilon RI signaling pathway	Endometrial cancer
Cell adhesion molecules (CAMs)	**GENETIC INFORMATION PROCESSING**	Fc gamma R-mediated phagocytosis	Glioma
Jak-STAT signaling pathway	Aminoacyl-tRNA biosynthesis	GnRH signaling pathway	Hypertrophic cardiomyopathy (HCM)
mTOR signaling pathway	Basal transcription factors	Insulin signaling pathway	Melanoma
Neuroactive ligand-receptor interaction	Non homologous end-joining	Leukocyte transendothelial migration	Non-small cell lung cancer
TGF-beta signaling pathway	Proteasome	Long-term depression	Pancreatic cancer
	RNA degradation	Long-term potentiation	Parkinson's disease
	Spliceosome	Melanogenesis	Pathways in cancer
	Ubiquitin mediated proteolysis	Natural killer cell mediated cytotoxicity	Primary immunodeficiency
		Olfactory transduction	Prostate cancer
		Renin-angiotensin system	Renal cell carcinoma
		T cell receptor signaling pathway	Small cell lung cancer
		Toll-like receptor signaling pathway	Thyroid cancer
		Vascular smooth muscle contraction	Type II diabetes mellitus

Table 3. The 70 pathways containing the 60 genes mapped by Pathway Express.

	Genes	Fold-Change direction
Lipoprotein functions	Ldlrap1 (LDL receptor adaptor protein 1)	↑
	Lrp10 (low-density lipoprotein receptor-related protein10)	↑
	Apod (Apolipoprotein D)	↑
	Scarb1 (scavenger receptor class B, member 1)	↑
	Sirt6 (sirtuin 6)	↑
	Osbpl5 (oxysterol binding protein-like 5)	↑
Lipolysis and *Beta-oxidation*	Adra2c (adrenergic, alpha-2C-, receptor)	↓
	G0s2 (G(0)/G(1) switch gene 2)	↓
	Acsl5 (acyl-CoA synthetase long-chain family member 5)	↑
	Pex5 (peroxisomal biogenesis factor 5)	↑
Adipogenesis	Stat5b (signal transducer and activator of transcription 5B)	↑
	Cebpb (CCAAT/enhancer binding protein (C/EBP), beta)	↓
	Pmp22 (peripheral myelin protein 22)	↑
	Sirt2 (sirtuin 2)	↑
	Nolc1 (nucleolar and coiled-body phosphoprotein 1)	↓
	Igfbp2 (insulin-like growth factor binding protein 2)	↓
	Dmpk (dystrophia myotonica-protein kinase)	↑
	Apln (apelin),	↓
	Paqr3 (progestin and adipoQ receptor family member III)	↑
	Pla2g2a (phospholipase A2, group IIA (platelets, synovial fluid)	↓

Table 4. Genes identified using the information contained in OntoExpress, GeneCards, PubGene and Coremine bioinformatics tools.

RT-qPCR RESULTS

In order to validate the microarray results, six genes differentially expressed between T_1AM treated and untreated rats were selected for the RT-qPCR analysis: Scarb1, Acsl5, Hdlbp, Apod, Igfbp2, and Cebpb. All these genes were chosen both for their p-value and biological relevance. The differential expression was confirmed for Igfbp2, Acsl5, Scarb1 and Apod genes. Cebpb showed the same trend of differential expression evidenced by microarrays but without reaching any statistical significance. The differential expression of Hdlbp was opposite to that observed by microarrays and not statistically significant (figure 6).

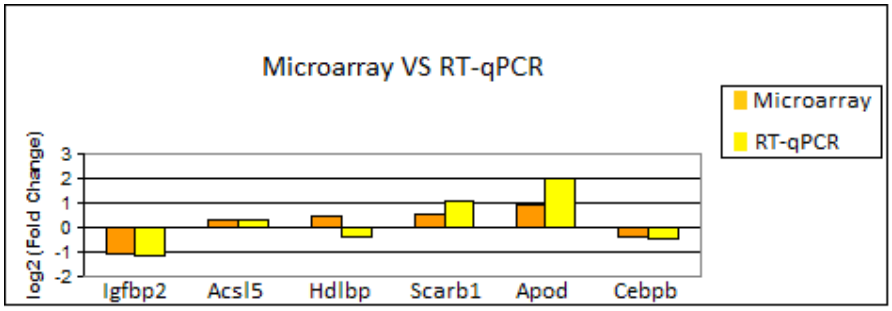

Figure 6. The differential expression of six genes, observed by microarrays, was checked by RT-$_q$PCR. Changes in gene expression were confirmed for four of these genes: Igfbp2, Acsl5, Scarb1 and Apod. The trend of differential expression evidenced by microarrays was confirmed for Cebpb but not for Hdlbp gene.

DISCUSSION

T_1AM slows down the metabolism by blocking carbohydrate utilisation and promoting lipid consumption (Braulke et al. 2008). The molecular mechanism by which T_1AM favours lipid over glucose catabolism is not known. However considering the lasting effects of T_1AM on fatty acid metabolism (Braulke et al. 2008), it is reasonable to expect that the observed shift in energy utilization arises from changes in gene expression.

In order to investigate the molecular mechanisms underlying the metabolic effects of T_1AM, gene expression profiles were analyzed in the subcutaneous adipose tissue of eight rats chronically treated with T_1AM as compared with eight untreated rats..

Three hundreds and 78 genes resulted differentially expressed. Sixty of them were mapped in 70 pathways by Pathway Express. This limited number of mapped genes depends on the fact that the information currently present in KEGG (Kyoto Encyclopedia of Genes and Genomes), the genomic bank on which Pathway Express relies, is still incomplete.

Of the 70 retrieved pathways, as metabolic pathways are not included in Pathway Express, only three, contribute to explain the T_1AM effect on metabolism: the adipocytokine signalling pathway, the insulin signalling pathway and the phosphatidylinositol signalling pathway. In addition, many of these pathways were identified by just one mapped gene, which makes their actual regulation by T_1AM difficult to prove..

As a result the pathway analysis was integrated with data obtained by OntoExpress, GeneCards, PubGene and Coremine bioinformatics tools. This made it possible to identify other 20 genes implicated in molecular mechanisms relevant to the T1AM metabolic effect.

T_1AM UP-REGULATES GENES RELATED TO LIPOPROTEIN FUNCTION

Lipoproteins are delegated to transport lipids, which are insoluble in blood, in the circulatory system. They are spherical particles with a core composed of cholesterol esters (CE) and triacylglicerols. Their surface is composed of amphiphilic proteins and lipids whose outward-facing surfaces are water-soluble and inward-facing surfaces are lipid-soluble. Most of the adipocyte cholesterol originates from circulating lipoproteins (Yu, Zhao and Hu 2010). *D*e *novo* synthesis of cholesterol is, in fact, low in the adipose tissue, as observed in early studies which reported that the rate of cholesterol synthesis in fat cells is only 4% of that of liver (Kovanen, Nikkilä and Miettinen 1975).

Some genes regulated by T_1AM are related to lipoprotein function and five of them are of particular interest: **Ldlrap1** (LDL receptor adaptor protein 1)**, Lrp10** (low-density lipoprotein receptor-related protein10), **Apod** (Apolipoprotein D), **Scarb1** (scavenger receptor class B, member 1), **Sirt6** (sirtuin [silent mating type information regulation 2 homolog] 6).

The **Ldlrap1** product is an adaptor protein required for efficient endocytosis of low density lipoprotein receptor (LDLR), which plays a crucial role for the removal of circulating LDLs (Low Density Lipoproteins) (Michaely et al. 2004). LDLs are the main cholesterol-transporting lipoproteins in plasma (Mahley et al. 1984). The protein encoded by this gene stabilizes the association between LDLR and LDL and promotes the internalization of the LDL-LDLR complex (Michaely et al. 2004).

Alterations in the bond between LDL and LDLR impede the endocytosis of the complex and lead to an accumulation of LDL in plasma. Elevated plasma levels of LDL are a key risk factor for the onset of coronary artery disease (Ross 1986).

Lrp10 belongs to the LDLR family and its product mediates the cellular uptake of VLDLs (Very Low Density Lipoproteins) remnants *in vitro* (Sugiyama et al. 2000). VLDLs are lipoproteins produced by the liver, rich in triglycerides and relatively poor in cholesterol. Nascent VLDLs are released from the liver into the bloodstream and the triglycerides are hydrolysed by lipoprotein lipase (LPL). The released fatty acids are used by the adipose and muscle tissues for storage or energy production. The VLDLs, depleted of triglycerides and enriched with cholesterol, are called VLDL remnants and are degraded by the liver. Sugiyama and colleagues demonstrated that LRP10, through the interaction with apoE which is abundant in the VLDL remnants, is involved in their blood clearance (Sugiyama et al. 2000). Lrp10 is also a molecular target of Ginko Biloba that is known to have cholesterol-lowering effect (Xie et al. 2009).

Apod is an apolipoprotein structurally similar to the lipocalin family proteins that is responsible for lipid transport. A reduced Apod expression alters the lipid metabolism (Perdomo and Henry Dong 2009). Plasma Apod is a component of HDLs (High Density Lipoproteins) involved in the "reverse cholesterol transport" by which the cholesterol is transferred from peripheral tissues to the liver for biliary excretion (Mahley et al. 1984). Apod modulates the activity of lecithin:cholesterol acyltransferase (LCAT), an HDL-bound enzyme that catalyzes the conversion of free cholesterol to CE that is then recruited into the HDL core. An increase in the cholesterol esterification by LCAT is observed in presence of Apod and the formation of Apod-LCAT complex has a stabilizing effect on LCAT (Steyrer and Kostner 1988). By enhancing the cholesterol esterification through LCAT, Apod indirectly promotes the reverse cholesterol

transport (Rassart et al. 2000). Moreover, a covalent cross-link between Apod and Apoa-II, a structural component of HDL, has been identified (Blanco-Vaca et al. 1992).

In the adipocytes, Apod is a target for liver X receptor (LXR) that recognizes cellular cholesterol in excess (Hummasti et al. 2004, Lehmann et al. 1997). In particular, LXR protects the cells from cholesterol accumulation, by the activation of the reverse cholesterol transport (Crestani et al. 2004).

The **Scarb1** gene codifies an HDL transmembrane receptor that mediates CE transfer from plasma HDL to tissues without HDL particle degradation (CE selective up-take) (Acton et al. 1996). The protein has horseshoe-like membrane topologies with a large extracellular loop anchored to the plasma membrane at both the N- and C- extremities (Krieger 2001).

HDL-Scarb1 interaction induces the formation of an hydrophobic channel by which the HDL unloades the CE. The cholesterol-depleted HDL comes off the receptor and re-enters in circle to capture other molecules of peripheral cholesterol (Trigatti, Rigotti and Krieger 2000).

Given that Scarb1 regulates the cholesterol levels into plasma HDL, its decrease has been associated with increased susceptibility to atherosclerosis: Scarb1 KO mice show elevated HDL cholesterol plasma levels and reduced selective HDL cholesterol clearance(Rigotti et al. 1997, Out et al. 2004). In addition, the distruption of Scarb1 gene in atherosclerotic mice (APOE $^{-/-}$) accelerates the onset of atherosclerosis (Trigatti et al. 1999). These studies suggest a protective effect of Scarb1 toward atherosclerosis.

Sirt6 codifies a member of sirtuin family that has NAD-dependent deacetylase and ADP-ribosyltransferase activities (Blander and Guarente 2004, Haigis and Guarente 2006, Liszt et al. 2005). It has been recently observed that transgenic mice overexpressing Sirt6 and fed with high fat diet accumulate significantly less LDL-cholesterol compared with their wild–type littermates (Kanfi et al. 2010).

To summarize, T_1AM, by modulating the expression of genes related to lipoprotein function, seems to affect the cholesterol homeostasis. This hypothesis is corroborated by the upregulation of another gene, **Osbpl5** (oxysterol binding protein-like 5) which codifies a member of the oxysterol-binding protein (OSBP) family that controls the oxysterol activity (Beh et al. 2001). The oxysterols, oxygenated derivatives of cholesterol, are particularly potent inhibitors of cholesterol biosynthesis (Gill, Chow and Brown 2008).

T_1AM REGULATES GENES RELATED TO LIPOLYSIS AND BETA-OXIDATION

Lipolysis hydrolyzes triglycerides and releases glycerol and free fatty acids. It is a catabolic process that provides energy to the adipose tissue when needed. Some genes related to lipolysis, like **Adra2c** (adrenergic, alpha-2C-, receptor) and **G0s2** ((G(0)/G(1) switch gene 2)) are down-regulated by T_1AM.

Adra2c is a target of catecholamines that are important regulators of fat cell lipolysis (Langin 2006). Sustained lipid mobilization and an increase in energy expenditure were observed during administration of an alpha2-adrenoceptor antagonist in dogs and humans (Lafontan and Berlan 1995, Berlan, Montastruc and Lafontan 1992).

The **G0s2** protein negatively regulates the activity of the adipose triglyceride lipase (ATGL), which catalyzes the first step in the hydrolysis of triglycerides. G0s2 protein binds directly to ATGL and reduces ATGL-mediated lipolysis by inhibiting its hydrolase activity (Yang et al. 2010). In Hela cells, the G0S2 over-expression prevents the ATGL-mediated lipid droplet degradation as well as basal and stimulated lipolysis in cultured adipocytes, whereas the down-regulation of endogenous G0S2 enhances adipocyte lipolysis (Yang et al. 2010).

In addition, T_1AM up-regulates the expression of genes linked to beta-oxidation, like **Acsl5** (acyl-CoA synthetase long-chain family member 5) and **Pex5** (peroxisomal biogenesis factor 5).

In the cytoplasm, the free fatty acids coming from lipolysis are converted to acyl-CoA thioesters by the acyl-CoA synthetases (ACSs). Then, they are directed toward the *de novo* lipid synthesis to store energy or toward beta-oxidation both in mitochondria and in peroxisomes to produce ATP (Achouri et al. 2005). ACSs are classified based on their preference for short, medium, long and very long chain fatty acids (Coleman et al. 2002b). Long-chain ACSs (ACSLs) modify fatty acids long 12-22 carbons (Li 2006). The **Acsl5** is the only ACSL isoform known to be located on the mitochondrial outer membrane and has a probable role in the beta-oxidation of fatty acids (Coleman et al. 2002a). In support of this hypothesis an increase of Acsl5 protein and mRNA after food deprivation has been observed (Lewin et al. 2001). Moreover, Acsl1 and Acsl4 but not Acsl5 are inhibited by Triascin C (Kim, Lewin and Coleman 2001) that blocks the *de novo* triglyceride synthesis (Igal, Wang and Coleman 1997). This suggests that Acsl5 is not linked to the triglyceride synthesis.

The **Pex5** gene codes a protein involved in the biogenesis of peroxisomes, which are organelles where the initial steps of beta-oxidation of very long chain fatty acids occur (Varanasi et al. 1996, Mannaerts, Van Veldhoven and Casteels 2000). These data suggest that T_1AM promotes both triglyceride lipolysis and beta-oxidation, according to an increased lipid utilisation.

T_1AM REGULATES THE EXPRESSION OF GENES RELATED TO ADIPOGENESIS

The amount of body fat depends on several factors that affect both the size and the number of adipocytes. Besides mature adipocytes, the adipose tissue contains multipotent mesenchymal cells and pre-adipocytes able to proliferate after specific stimuli (Bon 2008). If the food intake exceeds the energy consumption, the mature adipocytes go towards hypertrophy (increase in size) and hyperplasia (increase in number) (Bon 2008). The hypertrophy arises from triglyceride accumulation in existing adipocytes. The hyperplasia, also known as adipogenesis, comes from recruitment, proliferation and differentiation of pre-adipocytes (Hausman et al. 2001).

Several transcription factors, including members of the C/EBP family, are induced during the adipocyte differentiation and play an important role in the regulation of adipocyte gene expression (Rosen et al. 2002). **Cebpb,** for example, down-regulated by T_1AM, is the first player in adipogenesis, being responsible of C/EBPalfa and PPARgamma activation (Miyaoka et al. 2006, Rosen et al. 2002).

The adipocyte gene expression is also affected by Signal Transducers and Activators of Transcription (STATs) (White and Stephens 2010). **Stat5b,** up-regulated by T_1AM, is activated in the early phase of the differentiation process and is a positive regulator of proliferation (Nanbu-Wakao et al. 2002). However, a continuous and excessive activation of Statb becomes inhibitory for the adipogenesis (Miyaoka et al. 2006).

Many other genes regulated by T1AM, including **Pmp22** (peripheral myelin protein 22), **Sirt2** (sirtuin [silent mating type information regulation 2 homolog] 2), **Nolc1** (nucleolar and coiled-body phosphoprotein 1) and **Igfbp2** (insulin-like growth factor binding protein 2, 36kDa) are implicated in the adipogenesis.

Pmp22, up-regulated by T_1AM, belongs to the Growth Arrest Specific (GAS) gene family. The genes of this family regulate the cellular growth by blocking the mitotic division in response to extracellular signals (Schneider, King and Philipson 1988). In mice 3T3-L1, during the pre-adipocyte maturation, the GAS genes are upregulated and the Pmp22 gene exerts an inhibitory effect on adipogenesis (Shugart et al. 1995).

Sirt2, up-regulated by T_1AM, codifies a member of the sirtuin family. In mouse 3T3-L1 pre-adipocytes, the Sirt2 overexpression inhibits the adipocyte differentiation (Jing, Gesta and Kahn 2007). Conversely, Sirt2 downexpression promotes the adipogenesis (Jing et al. 2007). Sirt2 suppresses the adipogenesis by deacetylating FOXO1, which ties PPARgamma and represses its transcriptional activity (Jing et al. 2007).

Nolc1, down-regulated by T_1AM, codifies a member of the retinoblastoma family. These proteins are phosphorilated by cyclins to promote cell proliferation in a variety of cells (Claudio, Tonini and Giordano 2002). In the adipose tissue, the cell proliferation is stimulated by FGF10 through the activation of the Ras/Map pathway followed by the cyclin D2-dependent NOLC1-phosphorylation (Konishi et al. 2006).

Igfbp2, down-regulated by T_1AM, codifies a member of the IGF binding protein family that sequesters the IGFs in the extracellular environment and limits their access to the signalling receptors (Baxter and Twigg 2009). In particular, Igfbp2 inhibits the IGF1-IGF1R interaction by sequestering IGF1 (Baxter and Twigg 2009) that is an inducer of pre-adipocyte differentiation (MacDougald and Lane 1995). Whether Igfbp2 exerts an inhibitory effect on pre-adipocyte differentiation by sequestering IGF1 is unknown (Baxter and Twigg 2009), but it has been recently observed that mice overexpressing Igfbp2 have an increase in fat mass compared to their nontransgenic littermates (Rehfeldt et al. 2010). These data raise the hypothesis that T_1AM controls the adipose tissue expansion by inhibiting adipogenesis.

The up-regulation of **Dmpk** (dystrophia myotonica-protein kinase) gene, instead, might contribute to control the adipose tissue increment by reducing the adipocyte hypertrophy. This gene encodes a serine/threonine protein kinase, whose deficiency appears to be a risk factor for adiposity. Dmpk KO mice fed with high-fat diet, in fact, exhibit increased body weight and fat mass compared to wild type mice. This increase in adipose tissue mass correlates with the adipocyte hypertrophy (Llagostera et al. 2009).

Finally, given that the adipose tissue expansion requires the formation of new vessels, (Christiaens and Lijnen 2010, Rupnick et al. 2002, Hausman and Richardson 2004) the regulation of angiogenesis-related genes, like **Apln** (apelin), **Paqr3** (progestin and adipoQ receptor family member III) and **Pla2g2a** (phospholipase A2, group IIA platelets, synovial fluid) might represent a molecular mechanism by which T_1AM inhibits the adipogenesis.

Apln gene, down-regulated by T_1AM, encodes a peptide binding the APJ receptor (Tatemoto et al. 1998) and promotes angiogenesis in several tissues (Cox et al. 2006, Brooks, Clark and Cheresh 1994, Sorli et al. 2007). Kunduzova and colleagues demonstrated that the apelin/APJ signalling pathway promotes the angiogenesis also in the adipose tissue (Kunduzova et al. 2008). It has been proposed that the block of apelin signalling decreases angiogenesis and adiposity (Rayalam et al. 2008).

Paqr3 gene, up-regulated by T_1AM, codifies an adiponectin receptor (Garitaonandia et al. 2009) that has been reported to inhibit the angiogenesis by suppressing the VEGF signalling both in vitro and in vivo (Zhang et al. 2010).

Pla2g2a gene, down-regulated by T_1AM, codifies a phospholipase that catalyzes the sn-2 acyl-hydrolysis of phospholipids, thus causing the liberation of arachidonic acid that can be used to produce eicosanoids (Dennis 1997, Mayer and Marshall 1993). The Pla2g2a inhibition has been shown to reduce the formation of capillary-like tubes(Chen et al. 2004).

CONCLUSIONS

The results of this study suggest that T1AM controls the adipose tissue expansion by regulating genes linked to lipid metabolism, adipogenesis and angiogenesis. The observed changes in gene expression also contribute to explain the long lasting effects of T1AM on energy production, caused by a shift from carbohydrates to lipid metabolism. These findings furthermore suggest that T_1AM represents a good candidate for obesity treatment. In fact, not only it does not show the same negative side effects of thyroid hormones, but also influences the expression of genes able to control the blood cholesterol level. This provides new insights for the T_1AM action, like i.e. a protective role against atherosclerosis and coronary disease. These hypotheses are worthy to be further investigated by functional studies *in vitro* and *in vivo.*.

REFERENCES

Achouri, Y., B. D. Hegarty, D. Allanic, D. Bécard, I. Hainault, P. Ferré & F. Foufelle (2005) Long chain fatty acyl-CoA synthetase 5 expression is induced by insulin and glucose: involvement of sterol regulatory element-binding protein-1c. *Biochimie,* 87**,** 1149-55.

Acton, S., A. Rigotti, K. T. Landschulz, S. Xu, H. H. Hobbs & M. Krieger (1996) Identification of scavenger receptor SR-BI as a high density lipoprotein receptor. *Science,* 271**,** 518-20.

Baxter, R. C. & S. M. Twigg (2009) Actions of IGF binding proteins and related proteins in adipose tissue. *Trends Endocrinol Metab,* 20**,** 499-505.

Beh, C. T., L. Cool, J. Phillips & J. Rine (2001) Overlapping functions of the yeast oxysterol-binding protein homologues. *Genetics,* 157**,** 1117-40.

Benjamini, Y. & Y. Hochberg (1995) Controlling the false discovery rate: a practical and powerful approach to multiple testing. *J Roy Stat Soc Ser B (Meth),* 57**,** 289-300.

Berlan, M., J. L. Montastruc & M. Lafontan (1992) Pharmacological prospects for alpha 2-adrenoceptor antagonist therapy. *Trends Pharmacol Sci,* 13**,** 277-82.

Blanco-Vaca, F., D. P. Via, C. Y. Yang, J. B. Massey & H. J. Pownall (1992) Characterization of disulfide-linked heterodimers containing apolipoprotein D in human plasma lipoproteins. *J Lipid Res,* 33**,** 1785-96.

Blander, G. & L. Guarente (2004) The Sir2 family of protein deacetylases. *Annu Rev Biochem,* 73**,** 417-35.

Bon, G. B. (2008) [Adipose tissue: a multifunctional organ]. *G Ital Cardiol (Rome),* 9**,** 23S-28S.

Braulke, L. J., M. Klingenspor, A. DeBarber, S. C. Tobias, D. K. Grandy, T. S. Scanlan & G. Heldmaier (2008) 3-Iodothyronamine: a novel hormone controlling the balance between glucose and lipid utilisation. *J Comp Physiol B,* 178**,** 167-77.

Brooks, P. C., R. A. Clark & D. A. Cheresh (1994) Requirement of vascular integrin alpha v beta 3 for angiogenesis. *Science,* 264**,** 569-71.

Chen, W., L. Li, J. Zhu, J. Liu, J. Soria, C. Soria & S. Yedgar (2004) Control of angiogenesis by inhibitor of phospholipase A2. *Chin Med Sci J,* 19**,** 6-12.

Chiellini, G., S. Frascarelli, S. Ghelardoni, V. Carnicelli, S. C. Tobias, A. DeBarber, S. Brogioni, S. Ronca-Testoni, E. Cerbai, D. K. Grandy, T. S. Scanlan & R. Zucchi (2007) Cardiac effects of 3-iodothyronamine: a new aminergic system modulating cardiac function. *FASEB J,* 21**,** 1597-608.

Christiaens, V. & H. R. Lijnen (2010) Angiogenesis and development of adipose tissue. *Mol Cell Endocrinol,* 318**,** 2-9.

Claudio, P. P., T. Tonini & A. Giordano (2002) The retinoblastoma family: twins or distant cousins? *Genome Biol,* 3**,** reviews3012.

Coleman, R. A., T. M. Lewin, C. G. Van Horn & M. R. Gonzalez-Baró (2002a) Do long-chain acyl-CoA synthetases regulate fatty acid entry into synthetic versus degradative pathways? *J Nutr,* 132**,** 2123-6.

Coleman, R. A., C. G. Van Horn, M. R. Gonzalez-Baro & T. M. Lewin (2002b) Long-chain acyl-CoA synthetase isoforms and their functions. *Research Signpost,* 37**,** 1-15.

Cox, C. M., S. L. D'Agostino, M. K. Miller, R. L. Heimark & P. A. Krieg (2006) Apelin, the ligand for the endothelial G-protein-coupled receptor, APJ, is a potent angiogenic factor required for normal vascular development of the frog embryo. *Dev Biol,* 296**,** 177-89.

Crestani, M., E. De Fabiani, D. Caruso, N. Mitro, F. Gilardi, A. B. Vigil Chacon, R. Patelli, C. Godio & G. Galli (2004) LXR (liver X receptor) and HNF-4 (hepatocyte nuclear factor-4): key regulators in reverse cholesterol transport. *Biochem Soc Trans,* 32**,** 92-6.

Darimont, C., D. Gaillard, G. Ailhaud & R. Negrel (1993) Terminal differentiation of mouse preadipocyte cells: adipogenic and antimitogenic role of triiodothyronine. *Mol Cell Endocrinol,* 98**,** 67-73.

Dennis, E. A. (1997) The growing phospholipase A2 superfamily of signal transduction enzymes. *Trends Biochem Sci,* 22**,** 1-2.

Dhillo, W. S., G. A. Bewick, N. E. White, J. V. Gardiner, E. L. Thompson, A. Bataveljic, K. G. Murphy, D. Roy, N. A. Patel, J. N. Scutt, A. Armstrong, M. A. Ghatei & S. R. Bloom (2009) The thyroid hormone derivative 3-iodothyronamine increases food intake in rodents. *Diabetes Obes Metab,* 11**,** 251-60.

Draghici, S., P. Khatri, P. Bhavsar, A. Shah, S. A. Krawetz & M. A. Tainsky (2003) Onto-Tools, the toolkit of the modern biologist: Onto-Express, Onto-Compare, Onto-Design and Onto-Translate. *Nucleic Acids Res,* 31**,** 3775-81.

Draghici, S., P. Khatri, A. L. Tarca, K. Amin, A. Done, C. Voichita, C. Georgescu & R. Romero (2007) A systems biology approach for pathway level analysis. *Genome Res,* 17**,** 1537-45.

Garitaonandia, I., J. L. Smith, B. R. Kupchak & T. J. Lyons (2009) Adiponectin identified as an agonist for PAQR3/RKTG using a yeast-based assay system. *J Recept Signal Transduct Res,* 29**,** 67-73.

Gill, S., R. Chow & A. J. Brown (2008) Sterol regulators of cholesterol homeostasis and beyond: the oxysterol hypothesis revisited and revised. *Prog Lipid Res,* 47**,** 391-404.

Haigis, M. C. & L. P. Guarente (2006) Mammalian sirtuins--emerging roles in physiology, aging, and calorie restriction. *Genes Dev,* 20**,** 2913-21.

Hauner, H., G. Entenmann, M. Wabitsch, D. Gaillard, G. Ailhaud, R. Negrel & E. F. Pfeiffer (1989) Promoting effect of glucocorticoids on the differentiation of human adipocyte precursor cells cultured in a chemically defined medium. *J Clin Invest,* 84**,** 1663-70.

Hausman, D. B., M. DiGirolamo, T. J. Bartness, G. J. Hausman & R. J. Martin (2001) The biology of white adipocyte proliferation. *Obes Rev,* 2**,** 239-54.

Hausman, G. J. & R. L. Richardson (2004) Adipose tissue angiogenesis. *J Anim Sci,* 82**,** 925-34.

Hummasti, S., B. A. Laffitte, M. A. Watson, C. Galardi, L. C. Chao, L. Ramamurthy, J. T. Moore & P. Tontonoz (2004) Liver X receptors are regulators of adipocyte gene expression but not differentiation: identification of apoD as a direct target. *J Lipid Res,* 45**,** 616-25.

Ianculescu, A. G., K. M. Giacomini & T. S. Scanlan (2009) Identification and characterization of 3-iodothyronamine intracellular transport. *Endocrinology,* 150**,** 1991-9.

Igal, R. A., P. Wang & R. A. Coleman (1997) Triacsin C blocks de novo synthesis of glycerolipids and cholesterol esters but not recycling of fatty acid into phospholipid: evidence for functionally separate pools of acyl-CoA. *Biochem J,* 324 (Pt 2)**,** 529-34.

Jenssen, T. K., A. Laegreid, J. Komorowski & E. Hovig (2001) A literature network of human genes for high-throughput analysis of gene expression. *Nat Genet,* 28**,** 21-8.

Jing, E., S. Gesta & C. R. Kahn (2007) SIRT2 regulates adipocyte differentiation through FoxO1 acetylation/deacetylation. *Cell Metab,* 6**,** 105-14.

Kanfi, Y., V. Peshti, R. Gil, S. Naiman, L. Nahum, E. Levin, N. Kronfeld-Schor & H. Y. Cohen (2010) SIRT6 protects against pathological damage caused by diet-induced obesity. *Aging Cell,* 9**,** 162-73.

Khatri, P., S. Draghici, G. C. Ostermeier & S. A. Krawetz (2002) Profiling gene expression using onto-express. *Genomics,* 79**,** 266-70.

Kim, J. H., T. M. Lewin & R. A. Coleman (2001) Expression and characterization of recombinant rat Acyl-CoA synthetases 1, 4, and 5. Selective inhibition by triacsin C and thiazolidinediones. *J Biol Chem,* 276**,** 24667-73.

Klieverik, L. P., E. Foppen, M. T. Ackermans, M. J. Serlie, H. P. Sauerwein, T. S. Scanlan, D. K. Grandy, E. Fliers & A. Kalsbeek (2009) Central effects of thyronamines on glucose metabolism in rats. *J Endocrinol,* 201**,** 377-86.

Konishi, M., T. Asaki, N. Koike, H. Miwa, A. Miyake & N. Itoh (2006) Role of Fgf10 in cell proliferation in white adipose tissue. *Mol Cell Endocrinol,* 249**,** 71-7.

Kovanen, P. T., E. A. Nikkilä & T. A. Miettinen (1975) Regulation of cholesterol synthesis and storage in fat cells. *J Lipid Res,* 16**,** 211-23.

Krieger, M. (2001) Scavenger receptor class B type I is a multiligand HDL receptor that influences diverse physiologic systems. *J Clin Invest,* 108**,** 793-7.

Krotkiewski, M. (2002) Thyroid hormones in the pathogenesis and treatment of obesity. *Eur J Pharmacol,* 440**,** 85-98.

Kunduzova, O., N. Alet, N. Delesque-Touchard, L. Millet, I. Castan-Laurell, C. Muller, C. Dray, P. Schaeffer, J. P. Herault, P. Savi, F. Bono & P. Valet (2008) Apelin/APJ signaling system: a potential link between adipose tissue and endothelial angiogenic processes. *FASEB J,* 22**,** 4146-53.

Lafontan, M. & M. Berlan (1995) Fat cell alpha 2-adrenoceptors: the regulation of fat cell function and lipolysis. *Endocr Rev,* 16**,** 716-38.

Langin, D. (2006) Adipose tissue lipolysis as a metabolic pathway to define pharmacological strategies against obesity and the metabolic syndrome. *Pharmacol Res,* 53**,** 482-91.

Lehmann, J. M., S. A. Kliewer, L. B. Moore, T. A. Smith-Oliver, B. B. Oliver, J. L. Su, S. S. Sundseth, D. A. Winegar, D. E. Blanchard, T. A. Spencer & T. M. Willson (1997) Activation of the nuclear receptor LXR by oxysterols defines a new hormone response pathway. *J Biol Chem,* 272**,** 3137-40.

Lewin, T. M., J. H. Kim, D. A. Granger, J. E. Vance & R. A. Coleman (2001) Acyl-CoA synthetase isoforms 1, 4, and 5 are present in different subcellular membranes in rat liver and can be inhibited independently. *J Biol Chem,* 276**,** 24674-9.

Li, L. 2006. Functions of Rat Acyl-CoA Synthetases in bacteria and mammalian cells. In *Department of Nutrition, School of Public Health.* University of North Carolina.

Lin, B. C. & T. S. Scanlan (2005) Few things in life are "free": cellular uptake of steroid hormones by an active transport mechanism. *Mol Interv,* 5**,** 338-40.

Liszt, G., E. Ford, M. Kurtev & L. Guarente (2005) Mouse Sir2 homolog SIRT6 is a nuclear ADP-ribosyltransferase. *J Biol Chem,* 280**,** 21313-20.

Llagostera, E., M. C. Carmona, M. Vicente, R. M. Escorihuela & P. Kaliman (2009) High-fat diet induced adiposity and insulin resistance in mice lacking the myotonic dystrophy protein kinase. *FEBS Lett,* 583**,** 2121-5.

MacDougald, O. A. & M. D. Lane (1995) Transcriptional regulation of gene expression during adipocyte differentiation. *Annu Rev Biochem,* 64**,** 345-73.

Mahley, R. W., T. L. Innerarity, S. C. Rall & K. H. Weisgraber (1984) Plasma lipoproteins: apolipoprotein structure and function. *J Lipid Res,* 25**,** 1277-94.

Mannaerts, G. P., P. P. Van Veldhoven & M. Casteels (2000) Peroxisomal lipid degradation via beta- and alpha-oxidation in mammals. *Cell Biochem Biophys,* 32 Spring**,** 73-87.

Mayer, R. J. & L. A. Marshall (1993) New insights on mammalian phospholipase A2(s); comparison of arachidonoyl-selective and -nonselective enzymes. *FASEB J,* 7**,** 339-48.

Michaely, P., W. Li, R. Anderson, J. Cohen & H. Hobbs (2004) The modular adaptor protein ARH is required for low density lipoprotein (LDL) binding and internalization but not for LDL receptor clustering in coated pits. *J Biol Chem,* 279**,** 34023-31.

Miyaoka, Y., M. Tanaka, T. Naiki & A. Miyajima (2006) Oncostatin M inhibits adipogenesis through the RAS/ERK and STAT5 signaling pathways. *J Biol Chem,* 281**,** 37913-20.

Nanbu-Wakao, R., Y. Morikawa, I. Matsumura, Y. Masuho, M. A. Muramatsu, E. Senba & H. Wakao (2002) Stimulation of 3T3-L1 adipogenesis by signal transducer and activator of transcription 5. *Mol Endocrinol,* 16**,** 1565-76.

Out, R., M. Hoekstra, J. A. Spijkers, J. K. Kruijt, M. van Eck, I. S. Bos, J. Twisk & T. J. Van Berkel (2004) Scavenger receptor class B type I is solely responsible for the selective uptake of cholesteryl esters from HDL by the liver and the adrenals in mice. *J Lipid Res,* 45**,** 2088-95.

Perdomo, G. & H. Henry Dong (2009) Apolipoprotein D in lipid metabolism and its functional implication in atherosclerosis and aging. *Aging (Albany NY),* 1**,** 17-27.

Piehl, S., T. Heberer, G. Balizs, T. S. Scanlan, R. Smits, B. Koksch & J. Köhrle (2008) Thyronamines are isozyme-specific substrates of deiodinases. *Endocrinology,* 149**,** 3037-45.

Pietsch, C. A., T. S. Scanlan & R. J. Anderson (2007) Thyronamines are substrates for human liver sulfotransferases. *Endocrinology,* 148**,** 1921-7.

Rassart, E., A. Bedirian, S. Do Carmo, O. Guinard, J. Sirois, L. Terrisse & R. Milne (2000) Apolipoprotein D. *Biochim Biophys Acta,* 1482**,** 185-98.

Rayalam, S., M. A. Della-Fera, P. A. Krieg, C. M. Cox, A. Robins & C. A. Baile (2008) A putative role for apelin in the etiology of obesity. *Biochem Biophys Res Commun,* 368**,** 815-9.

Regard, J. B., H. Kataoka, D. A. Cano, E. Camerer, L. Yin, Y. W. Zheng, T. S. Scanlan, M. Hebrok & S. R. Coughlin (2007) Probing cell type-specific functions of Gi in vivo identifies GPCR regulators of insulin secretion. *J Clin Invest,* 117**,** 4034-43.

Rehfeldt, C., U. Renne, M. Sawitzky, G. Binder & A. Hoeflich (2010) Increased fat mass, decreased myofiber size, and a shift to glycolytic muscle metabolism in adolescent male transgenic mice overexpressing IGFBP-2. *Am J Physiol Endocrinol Metab,* 299**,** E287-98.

Rigotti, A., B. L. Trigatti, M. Penman, H. Rayburn, J. Herz & M. Krieger (1997) A targeted mutation in the murine gene encoding the high density lipoprotein (HDL) receptor scavenger receptor class B type I reveals its key role in HDL metabolism. *Proc Natl Acad Sci U S A,* 94**,** 12610-5.

Rosen, E. D., C. H. Hsu, X. Wang, S. Sakai, M. W. Freeman, F. J. Gonzalez & B. M. Spiegelman (2002) C/EBPalpha induces adipogenesis through PPARgamma: a unified pathway. *Genes Dev,* 16**,** 22-6.

Ross, R. (1986) The pathogenesis of atherosclerosis-an update. *N Engl J Med,* 314**,** 488-500.

Roy, G., E. Placzek & T. S. Scanlan (2012) ApoB-100-containing lipoproteins are major carriers of 3-iodothyronamine in circulation. *J Biol Chem,* 287**,** 1790-800.

Rupnick, M. A., D. Panigrahy, C. Y. Zhang, S. M. Dallabrida, B. B. Lowell, R. Langer & M. J. Folkman (2002) Adipose tissue mass can be regulated through the vasculature. *Proc Natl Acad Sci U S A,* 99**,** 10730-5.

Saba, A., G. Chiellini, S. Frascarelli, M. Marchini, S. Ghelardoni, A. Raffaelli, M. Tonacchera, P. Vitti, T. S. Scanlan & R. Zucchi (2010) Tissue distribution and cardiac metabolism of 3-iodothyronamine. *Endocrinology,* 151**,** 5063-73.

Safran, M., V. Chalifa-Caspi, O. Shmueli, T. Olender, M. Lapidot, N. Rosen, M. Shmoish, Y. Peter, G. Glusman, E. Feldmesser, A. Adato, I. Peter, M. Khen, T. Atarot, Y. Groner & D. Lancet (2003) Human Gene-Centric Databases at the Weizmann Institute of Science: GeneCards, UDB, CroW 21 and HORDE. *Nucleic Acids Res,* 31**,** 142-6.

Scanlan, T. S., K. L. Suchland, M. E. Hart, G. Chiellini, Y. Huang, P. J. Kruzich, S. Frascarelli, D. A. Crossley, J. R. Bunzow, S. Ronca-Testoni, E. T. Lin, D. Hatton, R. Zucchi & D. K. Grandy (2004) 3-Iodothyronamine is an endogenous and rapid-acting derivative of thyroid hormone. *Nat Med,* 10**,** 638-42.

Schena, M., D. Shalon, R. W. Davis & P. O. Brown (1995) Quantitative monitoring of gene expression patterns with a complementary DNA microarray. *Science,* 270**,** 467-70.

Schneider, C., R. M. King & L. Philipson (1988) Genes specifically expressed at growth arrest of mammalian cells. *Cell,* 54**,** 787-93.

Shugart, E. C., A. S. Levenson, C. M. Constance & R. M. Umek (1995) Differential expression of gas and gadd genes at distinct growth arrest points during adipocyte development. *Cell Growth Differ,* 6**,** 1541-7.

Smyth, G. 2005. Limma: linear models for microarray data. In *Bioinformatics and Computational Biology Solutions using R and Bioconductor.,* eds. R. Gentleman, V. Carey, S. Dudoit, R. Irizarry & W. Huber, 397-420. New York: Springer.

Smyth, G. K. (2004) Linear models and empirical bayes methods for assessing differential expression in microarray experiments. *Stat Appl Genet Mol Biol,* 3**,** Article3.

Snead, A. N., M. S. Santos, R. P. Seal, M. Miyakawa, R. H. Edwards & T. S. Scanlan (2007) Thyronamines inhibit plasma membrane and vesicular monoamine transport. *ACS Chem Biol,* 2**,** 390-8.

Sorli, S. C., S. Le Gonidec, B. Knibiehler & Y. Audigier (2007) Apelin is a potent activator of tumour neoangiogenesis. *Oncogene,* 26**,** 7692-9.

Steyrer, E. & G. M. Kostner (1988) Activation of lecithin-cholesterol acyltransferase by apolipoprotein D: comparison of proteoliposomes containing apolipoprotein D, A-I or C-I. *Biochim Biophys Acta,* 958**,** 484-91.

Sugiyama, T., H. Kumagai, Y. Morikawa, Y. Wada, A. Sugiyama, K. Yasuda, N. Yokoi, S. Tamura, T. Kojima, T. Nosaka, E. Senba, S. Kimura, T. Kadowaki, T. Kodama & T. Kitamura (2000) A novel low-density lipoprotein receptor-related protein mediating cellular uptake of apolipoprotein E-enriched beta-VLDL in vitro. *Biochemistry,* 39**,** 15817-25.

Tatemoto, K., M. Hosoya, Y. Habata, R. Fujii, T. Kakegawa, M. X. Zou, Y. Kawamata, S. Fukusumi, S. Hinuma, C. Kitada, T. Kurokawa, H. Onda & M. Fujino (1998) Isolation and characterization of a novel endogenous peptide ligand for the human APJ receptor. *Biochem Biophys Res Commun,* 251**,** 471-6.

Trigatti, B., H. Rayburn, M. Viñals, A. Braun, H. Miettinen, M. Penman, M. Hertz, M. Schrenzel, L. Amigo, A. Rigotti & M. Krieger (1999) Influence of the high density lipoprotein receptor SR-BI on reproductive and cardiovascular pathophysiology. *Proc Natl Acad Sci U S A,* 96**,** 9322-7.

Trigatti, B., A. Rigotti & M. Krieger (2000) The role of the high-density lipoprotein receptor SR-BI in cholesterol metabolism. *Curr Opin Lipidol,* 11**,** 123-31.

Vandesompele, J., K. De Preter, F. Pattyn, B. Poppe, N. Van Roy, A. De Paepe & F. Speleman (2002) Accurate normalization of real-time quantitative RT-PCR data by geometric averaging of multiple internal control genes. *Genome Biol,* 3**,** RESEARCH0034.

Varanasi, U., R. Chu, Q. Huang, R. Castellon, A. V. Yeldandi & J. K. Reddy (1996) Identification of a peroxisome proliferator-responsive element upstream of the human peroxisomal fatty acyl coenzyme A oxidase gene. *J Biol Chem,* 271**,** 2147-55.

Venditti, P., G. Napolitano, L. Di Stefano, G. Chiellini, R. Zucchi, T. S. Scanlan & S. Di Meo (2011) Effects of the thyroid hormone derivatives 3-iodothyronamine and thyronamine on rat liver oxidative capacity. *Mol Cell Endocrinol,* 341**,** 55-62.

Viguerie, N., L. Millet, S. Avizou, H. Vidal, D. Larrouy & D. Langin (2002) Regulation of human adipocyte gene expression by thyroid hormone. *J Clin Endocrinol Metab,* 87**,** 630-4.

White, U. A. & J. M. Stephens (2010) Transcriptional factors that promote formation of white adipose tissue. *Mol Cell Endocrinol,* 318**,** 10-4.

Wood, W. J., T. Geraci, A. Nilsen, A. E. DeBarber & T. S. Scanlan (2009) Iodothyronamines are oxidatively deaminated to iodothyroacetic acids in vivo. *Chembiochem,* 10**,** 361-5.

Wu, S. Y., W. L. Green, W. S. Huang, M. T. Hays & I. J. Chopra (2005) Alternate pathways of thyroid hormone metabolism. *Thyroid,* 15**,** 943-58.

Xie, Z., X. Wu, C. Zhuang, F. Chen, Z. Wang, Y. Wang & X. Hua (2009) [Protective effects of Ginkgo biloba extract on morphology and function of retinal ganglion cells after optic nerve transection in guinea pigs]. *Zhong Xi Yi Jie He Xue Bao,* 7**,** 940-6.

Yang, X., X. Lu, M. Lombès, G. B. Rha, Y. I. Chi, T. M. Guerin, E. J. Smart & J. Liu (2010) The G(0)/G(1) switch gene 2 regulates adipose lipolysis through association with adipose triglyceride lipase. *Cell Metab,* 11**,** 194-205.

Yu, B. L., S. P. Zhao & J. R. Hu (2010) Cholesterol imbalance in adipocytes: a possible mechanism of adipocytes dysfunction in obesity. *Obes Rev,* 11**,** 560-7.

Zhang, Y., X. Jiang, X. Qin, D. Ye, Z. Yi, M. Liu, O. Bai, W. Liu, X. Xie, Z. Wang, J. Fang & Y. Chen (2010) RKTG inhibits angiogenesis by suppressing MAPK-mediated autocrine VEGF signaling and is downregulated in clear-cell renal cell carcinoma. *Oncogene,* 29**,** 5404-15.